Nanoindentation tests on diamond-machined silicon wafers

Jiwang Yan,[a] Hirokazu Takahashi, Jun'ichi Tamaki, and Xiaohui Gai
Department of Mechanical Engineering, Kitami Institute of Technology, Koen-cho 165, Kitami, Hokkaido 090-8507, Japan

Hirofumi Harada
Siltronic Japan Corporation, 3434 Shimata, Hikari, Yamaguchi 743-0063, Japan

John Patten
Manufacturing Engineering Department, Western Michigan University, 1903 West, Michigan Ave, Kalamazoo, Michigan 49008-5314

(Received 6 December 2004; accepted 7 April 2005; published online 29 April 2005)

Nanoindentation tests were performed on ultraprecision diamond-turned silicon wafers and the results were compared with those of pristine silicon wafers. Remarkable differences were found between the two kinds of test results in terms of load-displacement characteristics and indent topologies. The machining-induced amorphous layer was found to have significantly higher microplasticity and lower hardness than pristine silicon. When machining silicon in the ductile mode, we are in essence always machining amorphous silicon left behind by the preceding tool pass; thus, it is the amorphous phase that dominates the machining performance. This work indicated the feasibility of detecting the presence and the mechanical properties of the machining-induced amorphous layers by nanoindentation. © *2005 American Institute of Physics*.
[DOI: 10.1063/1.1924895]

Silicon is not only a dominant substrate material for the fabrication of microelectronic and micromechanical components but also an important infrared optical material.[1,2] The manufacturing of large-diameter silicon wafers by ultraprecision ductile machining technology has become a subject of concentrated research interests.[3–6] A bottleneck for ductile machining processes is the machining-induced subsurface damages to silicon substrates, which involve dislocations and phase transformations. A number of previous studies have confirmed the presence of amorphous phase within the near-surface layer of ductile-machined silicon wafers.[7–11]

The subsurface damages, especially the amorphous layer, will significantly influence the mechanical, optical, and electrical functions of silicon parts. Virtually all studies of machined silicon surfaces involve the evaluation of this amorphous layer by default, even if the investigators did not realize it or explain this phenomenon. For example, when considering micromechanical applications where surface contacts and/or frictions exist, the mechanical properties of the amorphous layer, such as hardness, elasticity, and plasticity, become very important. The subsurface damages also influence the subsequent wafer manufacturing processes. That is, a machining operation always involves multiple tool passes due to the cross feed; thus, with the exception of the first cut, all subsequent cuts are made upon an amorphous material and not the starting crystalline material. From this point of view, it is essential to clarify the mechanical properties of this amorphous layer. However, to date, most silicon machining processes are based on the properties of the diamond-cubic single-crystalline phase, and little effort has been placed on the machining-induced amorphous phase.

During the past decades, response of single-crystal silicon to micro/nanolevel indentation has received extensive attention.[12–23] Unlike other materials, silicon often shows characteristic features in indentation depth in the unloading part of the load-displacement curve, namely, pop out or elbow, depending on the unloading rate, angle of the indenter, maximum load, or indentation depth.[19–21] These interesting phenomena are believed to be related to high-pressure phase transformations occurring beneath the indenter, which are accompanied by a significant volume change, and the extrusion (elbow) or containment (pop out) of the high pressure phase.

In this article, we report the results of nanoindentation tests performed on ultraprecision ductile-machined silicon wafers. When performing nanoindentation on machined silicon wafers, the indentation behavior will be dominated by the machining-induced amorphous layer for low loads and shallow depths. This situation can be simply considered as a thin film of amorphous silicon formed on a pristine crystalline substrate. Therefore, if a suitable indentation load is used, it may be possible to detect the presence and the mechanical property of this amorphous layer by nanoindentation.

In our experiments, electric device grade *p*-type single-crystal silicon (100) wafers having a doping level of 1.33×10^{14} atoms/cm^3, were used as specimens. These wafers are 25.4 mm in diameter, 0.725 mm in thickness, and obtained with chemomechanical polished finishes. The wafers were fixed to a hydrostatic spindle by heat-softened wax and were machined by fly-cutting using a straight-nosed diamond cutting tool[24] on an ultraprecision diamond lathe, Toyoda AHP 20-25N. We used a cutting tool with a −60° rake angle and a 6° relief angle for experiment. The tool rake angle was set to more negative than the practically used tools (−20–−40°), for the purpose of generating a thicker subsurface damage layer.[25] Other machining conditions were undeformed chip thickness 100 nm, tool feed 14 μm/rev, cutting edge angle 0.4°, depth of cut 2 μm, and cutting speed

[a]Present address: Department of Nanomechanics, Tohoku University, Aramaki Aoba 6-6-01, Aoba-ku, Sendai, 980-8579, Japan; electronic mail: yanjw@pm.mech.tohoku.ac.jp

 © 2005 American Institute of Physics

Downloaded from Yan Laboratory, Keio University at http://www.yan.mech.keio.ac.jp. Redistribution is subject to copyright licence from the journal publisher.

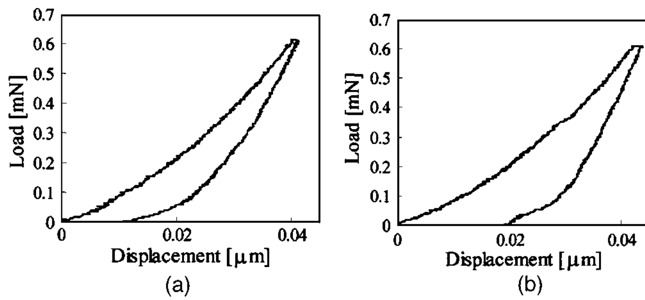

FIG. 1. Typical load-displacement curves in nanoindentation tests of (a) pristine silicon wafers and (b) machined silicon wafers.

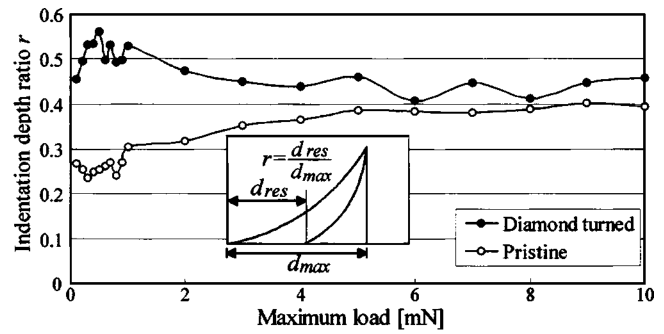

FIG. 3. Comparison of indentation depth ratio between the pristine silicon wafer and the machined silicon wafer.

15–18 m/s. Dry cutting was performed without any cutting fluid to avoid possible chemical effects.

One of these diamond-machined silicon wafers was used for preparing transmission electron microscope (TEM) samples by focused ion beam technique. The cross-sectional TEM micrographs of the machined silicon wafer showed that a 150 nm-thick amorphous layer was generated during machining, below which is a crystalline region with a few dislocations. The details of TEM observation will be addressed in another paper, together with selected area diffraction analysis.

A nanoindentation tester, ENT-1100a, produced by Elionix Co. Ltd. (Tokyo, Japan) was used for the present experiments. Tests were performed using a Berkovich-type diamond indenter. The circumferential orientation of the silicon wafer to the indenter was adjusted to make the orientation flat [110] parallel to one face of the indenter. The maximum load was varied in the range of 0.1–100 mN. The time for loading and unloading was the same and fixed to 5 s; thus, the loading/unloading rate changed in the range of 0.02–20 mN/s. Ten indentation tests were made for each experimental condition.

Typical load-displacement curves obtained in the experiments are shown in Fig. 1, where the maximum indentation load was 0.6 mN. During the indentation of pristine silicon, only elbows appeared on the unloading parts of the curves, as in Fig. 1(a). This is similar to previous results under fast unloading conditions, indicating a transformation from diamond cubic structure to amorphous.[19,20] However, for the machined silicon wafers under the same conditions, apart from elbows, pop outs were frequently observed during unloading, as shown in Fig. 1(b). Furthermore, on the loading parts of the load-displacement curves, pop-in phenomena were also observed.

At present, the physics governing the pop in and pop out in Fig. 1(b) is not yet clear. One of the possible factors might be the further phase transformations of the amorphous silicon, where further investigation is required to reach definitive conclusions.

Figure 2 is a comparison of measured hardness between the pristine silicon wafer and the machined silicon wafer. No remarkable difference was found when the maximum indentation load was larger than 0.6 mN. However, when the maximum load is smaller than 0.6 mN, the hardness of the diamond-turned silicon wafer becomes distinctly lower than that of the pristine silicon. At a sufficiently small load, the indentation response will be mainly due to the amorphous layer; thus, it can be concluded from these results that the machining-induced amorphous silicon is softer than diamond-cubic silicon. This surface-softening phenomenon is very different from conventional metal machining, where the near-surface layer always becomes harder due to the work-hardening effects. The work-hardening effect of metal is due to dislocation activities; while the surface-softening effect during silicon machining is caused by phase transformation.

Figure 3 is a comparison of indentation depth ratio between the pristine silicon wafer and the machined silicon wafer. Here we define the indentation depth ratio r as the ratio between the residual depth of the indent d_{res} and the maximum indentation displacement d_{max}. It is clear that the indentation depth ratio of the diamond-turned silicon wafer is higher than that of the pristine silicon, and this trend be-

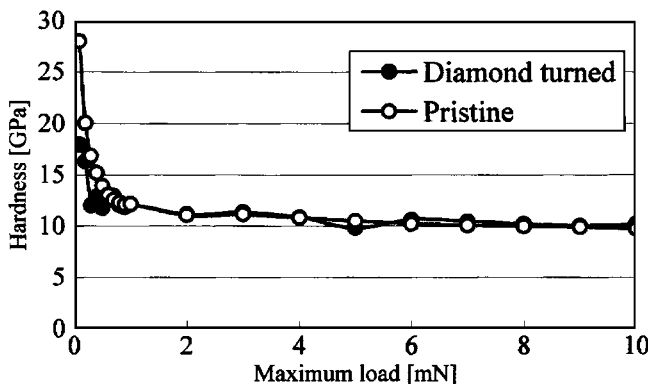

FIG. 2. Comparison of measured hardness between the pristine silicon wafer and the machined silicon wafer.

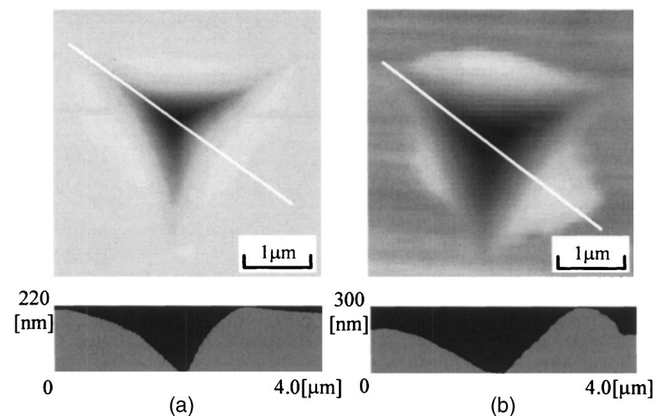

FIG. 4. AFM topographies and cross-sectional profiles of indents generated on (a) pristine silicon wafer and (b) machined silicon wafer.

comes stronger and stronger as the maximum load decreases. Because the indentation depth ratio r represents the degree of plastic deformation, the results in Fig. 3 indicate that the machining-induced amorphous silicon has significantly higher microplasticity than diamond-cubic silicon.

Figure 4 shows atomic force microscopic (AFM) topographies and cross-sectional profiles of the indents formed on pristine and machined silicon wafers, at a maximum load of 20 mN. In Fig. 4(a), the indent profile is extremely smooth, showing no evidence of protrusions. However, in Fig. 4(b), there are significant protrusions around the indent, which demonstrates that the amorphous layer has been subjected to significant plastic flow during indentation.

During loading with a Berkovich indenter on pristine silicon, the high pressure phase is constrained below the indenter by the near-surface diamond-cubic phase and cannot escape to the free surface to generate protrusions. Whereas when loading on the amorphous silicon, its random atom distribution would be easier to rearrange; thus, the high pressure phase can extend to the free surface allowing a pathway to extrude out from under the indenter.

As mentioned in the beginning, when machining silicon we are always working on an amorphous material as the preceding pass left behind in its wake an amorphous surface layer that the subsequent pass will encounter. Therefore, it is the microplascitity of the amorphous phase that in effect dominates the ductile machinability of silicon. From this aspect, we can say that when dealing with ductile machining technology the mechanical properties of the amorphous layer should be considered. This amorphous layer, if not completely removed, will also influence the surface function of produced silicon parts.

[1] S. G. Kaplan and L. M. Hanssen, Infrared Phys. Technol. **43**, 389 (2002).
[2] J. Yan, K. Syoji, and T. Kuriyagawa, J. Soc. Precis. Eng. **68**, 561 (2002).
[3] P. N. Blake and R. O. Scattergood, J. Am. Ceram. Soc. **73**, 949 (1990).
[4] T. Shibata, S. Fujii, E. Makino, and M. Ikeda, Precis. Eng. **18**, 130 (1996).
[5] J. Yan, K. Syoji, and T. Kuriyagawa, J. Soc. Precis. Eng. **65**, 1008 (1999).
[6] J. Yan, M. Yoshino, T. Kuriyagawa, T. Shirakashi, K. Syoji, and R. Komanduri, Mater. Sci. Eng., A **297**, 230 (2001).
[7] B. V. Tanikella, A. H. Somasekhar, A. T. Sowers, R. J. Nemanich, and R. O. Scattergood, Appl. Phys. Lett. **69**, 2870 (1996).
[8] T. Shibata, A. Ono, K. Kurihara, E. Makino, and M. Ikeda, Appl. Phys. Lett. **65**, 2553 (1994).
[9] C. Jeynes, K. E. Puttick, L. C. Whitmore, K. Gartner, A. E. Gee, D. K. Millen, R. P. Webb, R. M. A. Peel, and B. J. Sealy, Nucl. Instrum. Methods Phys. Res. B **118**, 431 (1996).
[10] K. E. Puttick, L. C. Whitmore, C. L. Chao, and A. E. Gee, Philos. Mag. A **69**, 91 (1994).
[11] J. Yan, J. Appl. Phys. **95**, 2094 (2004).
[12] I. V. Gridneva, Y. V. Milman, and V. I. Trefilov, Phys. Status Solidi A **14**, 177 (1972).
[13] V. G. Eremenko and V. I. Nikitenko, Phys. Status Solidi A **14**, 317 (1972).
[14] G. M. Pharr, W. C. Oliver, and D. S. Harding, J. Mater. Res. **6**, 1129 (1991).
[15] D. L. Callahan and J. C. Morris, J. Mater. Res. **7**, 1614 (1992).
[16] D. R. Clarke, M. C. Kroll, P. D. Kirchner, and R. F. Cook, Phys. Rev. Lett. **60**, 2156 (1988).
[17] A. Kailer, Y. G. Gogotsi, and K. G. Nickel, J. Appl. Phys. **81**, 3057 (1997).
[18] J. E. Bradby, J. S. Williams, J. Wong-Leung, M. V. Swain, and P. Munroe, Appl. Phys. Lett. **77**, 3749 (2000).
[19] V. Domnich, Y. Gogotsi, and S. Dub, Appl. Phys. Lett. **76**, 2214 (2000).
[20] H. Saka, A. Shimatani, M. Suganuma, and M. Suprijadi, Philos. Mag. A **82**, 1971 (2002).
[21] J. Jang, S. Wen, M. J. Lance, I. M. Anderson, and G. M. Pharr, Mater. Res. Soc. Symp. Proc. **795**, 313 (2004).
[22] I. Zarudi, J. Zou, and L. C. Zhang, Appl. Phys. Lett. **82**, 874 (2003).
[23] M. M. Khayyat, G. K. Banini, D. G. Hasko, and M M. Chaudhri, J. Phys. D **36**, 1300 (2003).
[24] J. Yan, K. Syoji, T. Kuriyagawa, and H. Suzuki, J. Mater. Process. Technol. **121**, 363 (2002).
[25] J. Yan, K. Syoji, and T. Kuriyagawa, J. Soc. Precis. Eng. **66**, 1130 (2000).